Long range lateral migration of intrinsic point defects in n-type 4H-SiC

L. S. Løvlie, , L. Vines, and , and B. G. Svensson

Citation: Journal of Applied Physics **111**, 103719 (2012); doi: 10.1063/1.4716181
View online: http://dx.doi.org/10.1063/1.4716181
View Table of Contents: http://aip.scitation.org/toc/jap/111/10
Published by the American Institute of Physics

Long range lateral migration of intrinsic point defects in n-type 4H-SiC

L. S. Løvlie, L. Vines, and B. G. Svensson
Department of Physics/Centre for Materials Science and Nanotechnology, P.O. Box 1048 Blindern, University of Oslo, N-0316 Oslo, Norway

(Received 15 December 2011; accepted 11 April 2012; published online 30 May 2012)

The lateral distributions of intrinsic point defects in n-type (0001) 4H-SiC have been investigated following room temperature irradiation with a focused beam of 10 keV protons. Laterally resolved deep level transient spectroscopy measurements reveal that the well-known and prominent $Z_{1/2}$ and $S_{1/2}$ centers display lateral diffusion lenghts on the order of 1 mm with negligible (if any) motion parallel to the direction of the c-axis. The migration occurs only in the presence of excess charge carriers generated during the proton irradiation, and no further motion takes place even under subsequent optical excitation of high intensity. Assuming one-dimensional geometry, an effective defect diffusivity in excess of 10^{-6} cm^2/s is deduced by numerical modelling of the experimental data, corresponding to an energy barrier for migration of ~0.2 eV. Possible mechanisms for the rapid migration, invoking charge carrier recombination as a necessary condition, are discussed, and especially, an association with the glide of partial dislocations along the (0001) basal plane is scrutinized in some detail. © *2012 American Institute of Physics*. [http://dx.doi.org/10.1063/1.4716181]

I. INTRODUCTION

Knowledge about defect evolution and diffusion in conjunction with activation of dopants and carrier lifetime control is among the most important reasons for studying intrinsic point defects in SiC. Several of the defects have, indeed, a detrimental effect on the concentration and lifetime of the charge carriers. In particular, the omnipresent $Z_{1/2}$ defect in 4H-SiC, exhibiting an acceptor level at ~0.7 eV below the conduction band edge (E_C),[1,2] has been identified to limit the bulk minority carrier lifetime in 4H-SiC bipolar devices.[3] $Z_{1/2}$ anneals out through multiple stages over a broad temperature range and it persists up to temperatures as high as ~2000 °C.[4] The multi-stage annealing implies reactions with other defects/impurities of limited concentration and which become mobile as the temperature increases until ultimately $Z_{1/2}$ itself becomes unstable. Moreover, it has previously been reported that certain point defects can migrate distances of several hundreds of micrometers during electron irradiation, as studied by photoluminescence (PL)[5,6] and deep level transient spectroscopy (DLTS).[7] The migration occurs laterally and an adverse effect on the use of implantation/irradiation for selective area doping and life-time control is anticipated. Specifically, carbon interstitials (C_I) were considered to migrate long distances, whereas Si vacancies largely remained confined within the directly irradiated volume.[5,6] Since the so-called $S_{1/2}$ levels at E_c – 0.45 eV and E_c – 0.72 eV (Ref. 8) and the $Z_{1/2}$ level were observed far away from the directly irradiated area,[7] it was suggested that C_I is involved in the formation of these centers. This was further supported by first-principles studies of antisite pairs in 4H-SiC, which unveiled that C_I (but not the carbon vacancy, V_C) can act as a catalyst for their formation during ionizing conditions, such as irradiation with energetic electrons and ions.[9]

In Refs. 6 and 7, it was speculated that the C_I's are able to migrate long distances through a diffusion process driven by successive changes in charge state, known as the Bourgoin-Corbett mechanism if no thermal activation is required (athermal process),[10] while a more normal ionization-enhanced (electronically stimulated) mechanism yields a lowering of the thermal energy required for motion. In the latter case, the ionization changes C_I from a rather immobile charge state with high energy barrier for migration to one which is relatively mobile with low migration barrier, i.e., the process remains thermally activated but with a reduced energy and the potential minimum position of C_i in the lattice is the same for the different charge states. In the former case, the potential minimum position of one charge state occurs at the saddle-point position for migration of the other charge state and vice versa; thus, by cycling between the charge states, the defect can move through the lattice without any thermal energy required. Several defects in other semiconductor materials have been considered to exhibit ionization-enhanced motion, like the self-interstitial in silicon,[10] the zinc interstitial in ZnSe (Refs. 11 and 12), and the oxygen dimer in silicon.[13,14] Especially, the latter one has been investigated extensively during the past decade since it is proposed to play a key role for light induced degradation of the minority carrier lifetime in silicon solar cells through formation of a substitutional boron–interstitial oxygen dimer complex, although this hypothesis has very recently been refuted.[15]

In the present work, we have studied in detail the lateral distribution of the $Z_{1/2}$ and $S_{1/2}$ defects in 4H-SiC following focused proton beam irradiation at room temperature (RT). Dramatic effects are observed with lateral migration distances on the order of millimeters. The experimental data are modelled assuming one-dimensional Fickian diffusion and effective diffusivity values are extracted. Possible

mechanisms for the long distance migration, which is highly anisotropic along the (0001) basal plane, are discussed. In particular, ionization-enhanced diffusion of the $Z_{1/2}$ and $S_{1/2}$ centers is ruled out as the only cause and arguments for the involvement of recombination-enhanced migration of extended defects, like gliding of partial dislocations along the basal plane, are put forward.

II. EXPERIMENT

Schottky barrier diodes (SBDs) were formed by electron-beam deposition of 100 nm thick circular Ni contacts (diameter = 400 μm) on n-type nitrogen doped (0001) 4H-SiC samples (purchased from Cree, Inc.) having a 10 μm thick epitaxial layer grown on the Si-face. The effective carrier concentration in the epitaxial layer was about 3×10^{15} cm^{-3}, while the substrate doping was about 10^{18} cm^{-3}. The concentrations of the $Z_{1/2}$ and $S_{1/2}$ defects were monitored by DLTS. The measurements were performed using an improved version of a custom made setup equipped with a HP 4280A capacitance bridge, described in detail elsewhere,[16] and a Semilab DLS83 setup, both having liquid nitrogen cryostats. Some selected measurements with high energy resolution were performed using a Boonton 7200 capacitance bridge and a closed-cycle helium cryostat.

Prior to the formation of SBDs and proton irradiation, the samples were thermally oxidized in dry O_2 at 1150 °C for 5 h and the resulting oxide layer was then removed in diluted HF. This procedure efficiently removes all deep-level defects with states in the upper half of the band gap,[17,18] thereby enhancing the sensitivity of the $Z_{1/2}$ and $S_{1/2}$ levels formed during the proton irradiation. This holds especially for the $Z_{1/2}$ level which is already present with a concentration of $\sim 10^{12}$ cm^{-3} in the as-grown material. The oxidation resulted in a 50 nm thick layer of SiO_2, indicating that a so-called trap eliminated depth of about 6 μm was obtained.[18] Except for enhancing the sensitivity, the oxidation has no influence on the observed long distance defect migration.[19] The proton irradiations were performed in a Cameca IMS 7f micro-analyzer, enabling positioning of the beam spot with an accuracy of less than 20 μm, using an energy of 10 keV and a focused beam with a diameter of $\sim$100 μm. The proton dose was about 4×10^{18} cm^{-2}, corresponding to an irradiation time of 1 h for a beam current of 10 nA, and the beam was positioned $\sim$50 μm away from the periphery of the nearest SBD. The irradiations were conducted at nominal room temperature with no significant heating of the samples.

III. RESULTS

A schematic illustration of the layout of SBDs on a sample is shown in Fig. 1. The contacts are arranged in a radial pattern, such that any possible dependency on the crystal orientation in the basal plane could be revealed. The beam was positioned in the region with the shortest distance between the 3 closest contacts to maximize the resolution for short migration distances, where the concentration is expected to change most rapidly. The irradiated area is visible due to discoloration caused by damage and strain in the irradiated region, illustrating the shape of the beam spot. The lateral

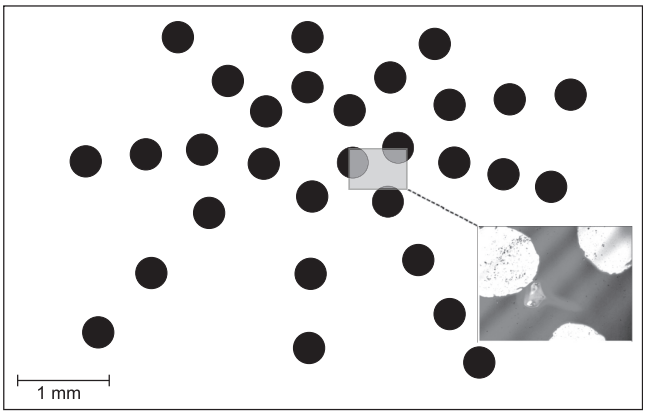

FIG. 1. An illustration of the layout of SBDs on a sample (inset). Close-up of the area indicated by the small rectangle, displaying the irradiated area and the closest contacts. The beam had an approximate diameter of 100 μm, with a tail towards the right in the image.

distance from the position of the beam to the center of each SBD varied from $\sim$250 μm up to 3.5 mm.

DLTS spectra were measured in the temperature range 150–350 K before and after irradiation, as shown in Fig. 2 for SBDs with increasing distance to the irradiated area. The DLTS peaks are broad but exhibit single-exponential Arrhenius behavior as shown in the inset, indicating that they are due to overlapping (discrete) energy levels. The properties of the detected peaks are summarized in Table I. The projected range of the 10 keV protons is $\sim$100 nm according to simulations using the TRIM software,[20] whilst the depletion region at zero-bias voltage extends almost 1 μm below the Ni/SiC interface. Accordingly, a forward bias of +1.5 V was used during the DLTS pulsing (duration 50 ms), with a quiescent reverse bias of −1.0 V, in order to probe the proton-induced defects in the vicinity of the surface. No DLTS signals were detected using a pulsing bias of 0 V, showing that all of the

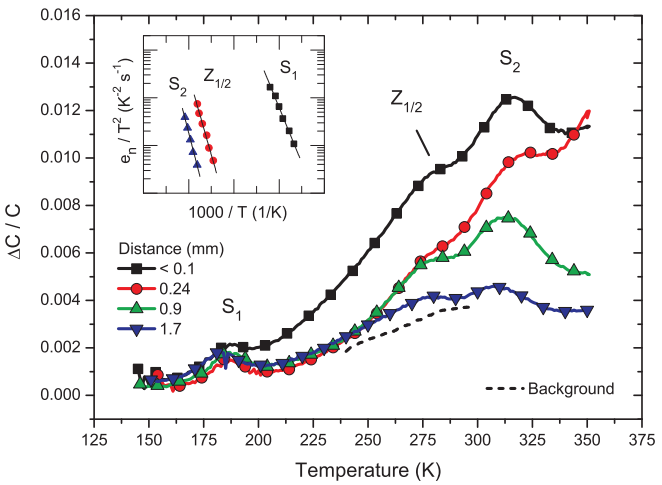

FIG. 2. DLTS spectra recorded before and after irradiation, showing the decrease in peak amplitudes with increasing distance from the irradiated area. Inset: Arrhenius plots for the DLTS peaks, showing that their emission rates (e_n), corrected for the temperature dependence of the electron velocity and of the density of states in the conduction band, depend exponentially on temperature, despite being rather broad. The DLTS spectra have a rate window of $(640 \text{ ms})^{-1}$ and are deduced using a weighting function of lock-in type.

TABLE I. The band gap position (±1 standard deviation) and apparent capture cross section (σ_a) of the trapping centers which are detectable in Fig. 2.

Trapping center	$E_C - E_t$ (eV)	σ_a (cm^2)
S_1	0.44 ± 0.01	3×10^{-14}
$Z_{1/2}$	0.65 ± 0.03	10^{-14}
S_2	0.77 ± 0.05	10^{-14}

detected defects occur no deeper than 1 μm below the surface. As illustrated in Fig. 2, a broad and featureless background signal exists prior to the irradiation originating from near-surface defects with rather deep states responding primarily at temperatures above 200 K.

Three levels are clearly discernible in Fig. 2; the S_1 level with a band gap position of $E_C - 0.44$ eV, $Z_{1/2}$ at $E_C - 0.65$ eV, and the S_2 level at approximately $E_C - 0.77$ eV. Employing a weighting function of GS4 type[21] with higher energy-resolution (but also more noise) than the one of lock-in type used in Fig. 2, the overlap between the three DLTS peaks becomes negligible (not shown). There is also at least one more level present just outside the measurement range ending at 350 K; this level was, however, not fully recorded in order to avoid unintentional annealing during the measurements. The DLTS peaks are quite broad, which is usually the case when monitoring the directly irradiated area immediately after bombardment with energetic electrons and ions at RT and before any annealing.[22] The identity of the $Z_{1/2}$ level has been discussed extensively in the literature for almost 15 years[2,23–30] and it is generally agreed to be C-related, but no full consensus has been reached on the atomic structure. The S_1 and S_2 levels are considered to be due to different charge states of the same defect center, since they frequently appear with similar concentrations after MeV electron and ion irradiation, anneal out in a close to 1:1 correspondence, and the shallowest level, S_1, exhibits a considerably smaller electron capture cross section than S_2.[8] The fact that the apparent capture cross section, σ_a, has comparable values for S_1 and S_2, Table I, implies a substantial entropy term ($\sim 4 \times 10^{-4}$ eV/K) for the S_1 charge state transition.[8]

The lateral distributions of the concentration of the $Z_{1/2}$ and S levels were mapped using 10 SBDs with increasing distance to the directly irradiated area and the results, corrected for the background contribution prior to irradiation, are depicted in Fig. 3. The distance is determined from the center of each SBD, and the data show that the average concentration of $Z_{1/2}$ and $S_{1/2}$, in the monitored depth interval decreases with increasing distance. Although the spacing and size of the contacts in comparison to the observed diffusion lengths allow only limited resolution in a given direction, no dependence on the crystal orientation could be detected. The decrease takes place over distances of $\leq$2 mm before reaching the detection limit of $\sim 1 \times 10^{12}$ cm^{-3}. Annealing for 1 h at 250 °C in dry air reduces the absolute concentration values by ~50%, without affecting the shape of the lateral distribution, and after 2 h, they are below the detection limit. Results reported in Ref. 19 from an independent experiment, where the $Z_{1/2}$ concentration was monitored at a fixed distance from the irradiated area, agree closely with the corresponding values in Fig. 3 demonstrating a high reproducibility of the experiments.

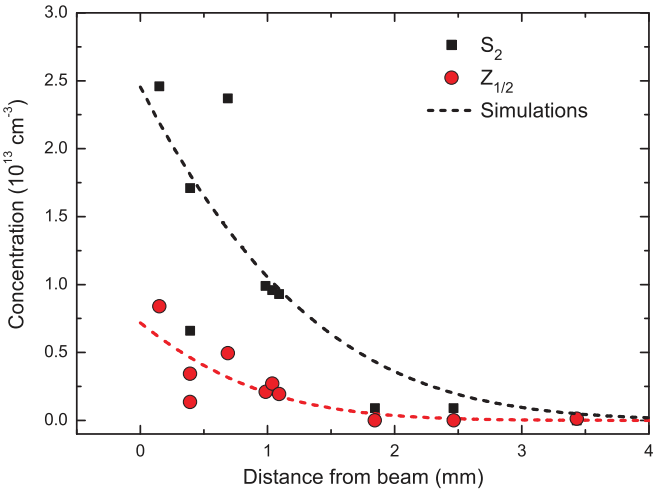

FIG. 3. Concentration versus distance from the irradiated area for the $Z_{1/2}$ and S_2 levels (revealed in Fig. 2). The DLTS background signal has been subtracted and one-dimensional diffusion has been assumed to fit the experimental data.

The data for the $Z_{1/2}$ and S_2 levels in Fig. 3 have been modelled assuming one-dimensional diffusion with a constant diffusivity, as described in detail in the following discussion section. The lateral diffusion length, defined as the distance from the irradiated area where the concentration is reduced to 1/e, becomes approximately 0.8 mm for $Z_{1/2}$ and 1.1 mm for S_2.

IV. DISCUSSION

The experimental data in Fig. 3 are compared with simulations employing the diffusion equation,

$$\frac{\partial N_t}{\partial t} = D_{eff} \frac{\partial^2 N_t}{\partial x^2}, \quad (1)$$

where N_t is the defect concentration, D_{eff} is the effective diffusivity at RT (considered to be constant as a function of time and distance), and x is the lateral distance from the irradiated area. The fitting was accomplished by varying D_{eff} and the generation rate of defects, J (in units of defects/cm^2 s). The generation rate J is estimated according to Fick's first law, which was used as the natural boundary condition at the area irradiated directly by the beam,

$$J(x = 0, t) = -D_{eff} \left(\frac{\partial N_t}{\partial x} \right)_{x=0}. \quad (2)$$

The boundary condition at large distances from the directly irradiated area is a vanishing defect concentration ($N_t(x = \infty, t) = 0$), in accordance with the experimental data showing no defect concentration above the detection limit after oxidation and prior to irradiation.

The time of diffusion was put equal to the irradiation time (1 h), as substantiated by the fact that no further migration was observed after termination of the irradiation; the measured defect distributions remained constant for >6

TABLE II. Survey of the parameters for defect migration as extracted from solving Eq. (1) and fitting the experimental data for $Z_{1/2}$, and S_2.

Defect	D_{eff} (10^{-6} cm^2/s)	J (10^{11} cm^{-2} s^{-1})	Migration length (mm)
$Z_{1/2}$	2	0.3	0.8
S_2	4	2.9	1.1

months after irradiation keeping the samples at RT. D_{eff} and J were varied over a broad range, and Eq. (1) was solved numerically for each set of (D_{eff}, J) until the values yielding the least squared error were found. In the case of $Z_{1/2}$, the best fit was obtained for $D_{eff} = 2 \times 10^{-6}$ cm^2/s and $J \approx 3 \times 10^{10}$ cm^{-2} s^{-1}, while for S_2, the corresponding values were $D_{eff} = 4 \times 10^{-6}$ cm^2/s and $J \approx 2.9 \times 10^{11}$ cm^{-2} s^{-1}. These diffusivities correspond to an energy barrier for migration on the order of 0.2 eV assuming a pre-exponential factor with a typical value of 10^{-2}–10^{-3} cm^2/s. The migration parameter values extracted from the simulations are summarized in Table II.

Here, it should be emphasized that the extracted values for J do not account for defects trapped within the directly irradiated volume but do account for dynamic annealing (self-recombination); assuming a threshold energy of 20 eV for displacement of C and Si atoms and neglecting dynamic annealing, the total generation rate of V_C, C_I, V_{Si}, and Si_I, becomes $\sim 10^{16}$ cm^{-2} s^{-1} for the experimental conditions used, according to an estimate based on TRIM calculations.[20] If ~1%–3% of the defects survive dynamic annealing,[31] this estimate implies that <1% of the surviving defects escape the directly irradiated volume and display long distance migration. This can perhaps be regarded as a small fraction but for sufficiently high doses of ion implantation (equivalent to $>10^{16}$ H/cm^2 in terms of damage formation), detrimental effects may be expected on the minority carrier lifetime in areas located several hundreds of μm away from the directly implanted one.

The values deduced for D_{eff} are high and imply rapid migration of the species involved. The process is highly anisotropic with respect to the c-plane, and only a very minor (if any) migration takes place along the direction parallel to the c-axis. Further, simultaneous irradiation is a necessary condition for the migration to occur and as discussed in Refs. 6 and 7, and 19, it is tempting to invoke ionization-enhanced motion of point defects as a possible cause for the observed effect. According to results from TRIM calculations,[20] one 10-keV-proton gives on average rise to ~2000 electron-hole pairs (EHP), assuming an average ionization energy of ~5.0 eV to generate an EHP in 4H-SiC.[32] If the minority carrier life time is put equal to 0.1 μs in the irradiated volume, i.e., about a factor 10 lower than that in as-grown high-purity epitaxial layers, and the carrier diffusivity is taken as ~1 cm^2/s (also about a factor 10 lower than in undamaged epitaxial layers), one obtains a carrier diffusion length of a few μm and a steady-state-density of $\sim 10^{15}$ EHP/cm^3 during the irradiation. This density is of the same order of magnitude as the free electron concentration in the epitaxial layer suggesting that the availability of holes is a limiting factor for the migration process.

In principle, the migrating species may be the $Z_{1/2}$ and $S_{1/2}$ defects themselves, one (or more) of their constituents or a "catalyst" species emerging from the directly irradiated volume and reacting with C/Si atoms in the unirradiated volume. The $Z_{1/2}$ center is commonly agreed on to be C-related,[24–27,29] and an obvious candidate for the rapidly migrating species is C_I;[6,7] in fact, first-principles density calculations by Eberlein *et al.*[9] show that the atomic structure of C_I, as well as of Si_I, is charge state dependent and migration can be enhanced by ionizing radiation. In particular, a mechanism for the production of antisite defects in 4H-SiC has been predicted where the supply of excess holes during irradiation of n-type material is decisive. If a C_I is generated and migrates to a Si site, the reaction $(C_I)_{Si} \rightarrow C_{Si} + Si_I$ is endothermic by ~5.9 eV for neutral defects and will not occur. However, if two holes are trapped by $(C_I)_{Si}$, the reaction becomes endothermic by only 0.6 eV, according to defect formation energies, and will take place with a substantial rate at RT assuming negligible additional reaction barriers. After rapid neutralization of the ejected Si_I^{2+} by capturing of two electrons, it can migrate to a C site and by capturing of one hole, the reaction $(Si_I)_C \rightarrow Si_C + C_I$ is endothermic by only ~0.2 eV relative to 1.8 eV for neutral defects.

Interestingly, the reaction enthalpies estimated by Eberlein *et al.*[9] are rather close to the migration barrier values extracted from the present experiment and may be regarded as an argument in favour of ionization-enhanced motion of C_I. On the other hand, the diffusion lengths of ~1 mm for $Z_{1/2}$ and $S_{1/2}$ in Fig. 3 are at least one order of magnitude higher than the average charge carrier diffusion length anticipated in epitaxial 4H-layers, suggesting that ionization-enhanced motion of C_I plays a limited role. Furthermore, exposure of the proton-irradiated samples to UV-irradiation, from a pulsed laser operating at 372 nm wavelength or a Hg lamp (output power centered around 365 nm wavelength), for a duration of 24 h and a steady-state injection of 10^{15} EHP/cm^3 did not cause any measurable diffusion of $Z_{1/2}$ and $S_{1/2}$. In addition, the pronounced anisotropy of the defect migration along the c-plane is not readily accounted for by ionization-enhanced motion of C_I.

The DLTS peaks in Fig. 2 are broad and do not originate from well-defined (unperturbed) but rather distorted $Z_{1/2}$ and $S_{1/2}$ centers. Similar spectra are also commonly found after irradiation with MeV ions or electrons at RT when monitoring the directly irradiated area,[22] and the broadening has been attributed to a dense local elastic energy deposition by these projectiles (and their recoils) causing a distorted crystal structure in the vicinity of $Z_{1/2}$ and $S_{1/2}$. Such an origin of the distortion is not likely to hold for the present experiment where the defects are located several hundreds of μm away from the directly irradiated area and the shape of the peaks does not exhibit any variation with the migration distance. Here, it can also be noted that the peak amplitudes of S_1 and S_2 in Fig. 2 display a large deviation from a one-to-one correspondence, in contrast to that found in Ref. 8 and contradicting the main argument for assigning the two levels to different charge states of the same defect center. However, in analogy with the deviation from a one-to-one relation

between the DLTS peak amplitudes of the singly and doubly negatively charged divacancy center in ion-bombarded silicon crystals,[31,33,34] the present results for S_1 and S_2 imply a high local concentration of defects leading to volumes with partial compensation and depletion of free electrons, preventing complete filling of the shallow S_1 level during DLTS pulsing. In fact, the collected amount of information from the DLTS data, e.g., the broad $Z_{1/2}$ and $S_{1/2}$ peaks relative to those of isolated point defects, that the $Z_{1/2}$ and $S_{1/2}$ peaks remain broad several hundreds of μm away from the irradiation volume, the strong deviation from a one-to-one relation between the S_1 and S_2 peak amplitudes, and the highly anisotropic motion of $Z_{1/2}$ and $S_{1/2}$ along the (0001) basal plane with negligible migration parallel to the c-axis, provide compelling evidence for the involvement of extended defects (distorted crystal structure) in the long-distance migration of $Z_{1/2}$ and $S_{1/2}$, and a possible scenario is outlined below.

About 10 years ago, 4H-SiC PiN diodes were found to degrade during forward-bias operation when an electron-hole plasma was generated in the n-base.[35,36] The degradation was associated with formation of stacking faults in the active region of the diode and the properties of the partial dislocations responsible for the stacking fault formation were studied in detail by Galeckas *et al.*[37,38] employing optical emission microscopy. In particular, the velocity and activation energy for the glide of partials on the basal c-plane were determined and found to be up to $\sim 10^{-4}$ cm/s at RT and $\sim$0.27 eV, respectively, in the presence of charge carrier recombination. The glide process is strongly enhanced by the recombination; in the dark, i.e., without any recombination, the activation energy is $\sim$2.5 eV and the dislocations are practically immobile at RT. Indeed, there are several striking features corroborating an association of the long-distance migration of $Z_{1/2}$ and $S_{1/2}$ with the glide of partials: (i) charge carrier recombination is a necessary condition for both processes to take place at RT, (ii) a strong degree of anisotropy along the (0001) basal plane is found in both cases, (iii) comparable absolute distances are obtained, 1 h at RT yields a migration length on the order of 1 mm in both cases, (iv) the DLTS signatures are broad and suggest that the $Z_{1/2}$ and $S_{1/2}$ centers appear in a distorted crystal structure (e.g., in the vicinity of an extended defect), (v) the migration lengths of $Z_{1/2}$ and $S_{1/2}$ are about the same despite their different origin/identity, possibly indicating that the diffusion is promoted by an independent process not linked to a specific point defect like C_I, and (vi) the partials anneal out at temperatures above 200 °C (Ref. 39) consistent with the disappearance of the $Z_{1/2}$ and $S_{1/2}$ signals after 2 h at 250 °C.

An exact mechanism of interaction between the partial dislocations and the $Z_{1/2}$ and $S_{1/2}$ centers cannot be elucidated from the present data but a distinct possibility may be that $Z_{1/2}$ and $S_{1/2}$ bind to some site in the core of the partials. However, in spite of the features (i)–(vi), one should also point out that the association of the long distance migration of $Z_{1/2}$ and $S_{1/2}$ with the glide of partial dislocations is still to be regarded as tentative and further work needs to be pursued for an unambiguous conclusion.

V. SUMMARY

At RT, the prominent $Z_{1/2}$ and $S_{1/2}$ centers in 4H-SiC exhibit long distance lateral migration on the order of 1 mm outside the volume irradiated directly by a focused beam of 10 keV protons. The migration is rapid with an energy barrier of $\sim$0.2 eV and it is strongly anisotropic along the (0001) basal plane. The presence of electron-hole pair recombination is a necessary condition and the DLTS spectra provide strong evidence of a distorted crystal structure in the vicinity of the $Z_{1/2}$ and $S_{1/2}$ centers. Ionization-enhanced defect motion plays a decisive role but is possibly driven by extended defects, like gliding of partial dislocations on the basal plane, with $Z_{1/2}$ and $S_{1/2}$ as accompanying complexes rather than by specific point defects, like C_I. Despite a rather limited fraction of defects escaping from the directly irradiated volume ($\leq$1%), the results imply that the minority charge carrier lifetime is adversely affected over distances of several hundreds of μm in conjunction with selective area doping by ion implantation.

ACKNOWLEDGMENTS

The authors acknowledge gratefully financial support from the Norwegian Research Council under the FRINAT program (CAPSiC project), and are thankful to Dr. Augustinas Galeckas for the laser irradiations and for fruitful discussions.

[1]C. G. Hemmingsson, N. T. Son, A. Ellison, J. Zhang, and E. Janzén, Phys. Rev. B **58**, R10 119 (1998).
[2]T. Dalibor, G. Pensl, T. Kimoto, H. Matsunami, S. Sridhara, R. P. Devaty, and W. J. Choyke, Diamond Relat. Mater. **6**, 1333–1337 (1997).
[3]P. B. Klein, B. V. Shanabrook, S. W. Huh, A. Y. Polyakov, M. Skowronski, J. J. Sumakeris, and M. J. O'Loughlin, Appl. Phys. Lett. **88**, 52110 (2006).
[4]G. Alfieri, E. V. Monakhov, B. G. Svensson, and M. K. Linnarsson, J. Appl. Phys. **98**, 43518 (2005).
[5]J. W. Steeds, W. Sullivan, A. Wotherspoon, and J. M. Hayes, J. Phys.: Condens. Matter **21**, 364219 (2009).
[6]J. Steeds, G. A. Evans, L. R. Danks, S. Furkert, W. Voegeli, M. M. Ismail, and F. Carosella, Diamond Relat. Mater. **11**, 1923–1945 (2002).
[7]G. Alfieri, U. Grossner, E. V. Monakhov, B. G. Svensson, J. W. Steeds, and W. Sullivan, Mater. Sci. Forum **527–529**, 485–488 (2006).
[8]M. L. David, G. Alfieri, E. V. Monakhov, A. Hallen, C. Blanchard, B. G. Svensson, and J. F. Barbot, J. Appl. Phys. **95**, 4728 (2004).
[9]T. Eberlein, C. Fall, R. Jones, P. Briddon, and S. Öberg, Phys. Rev. B **65**, 1–4 (2002).
[10]J. C. Bourgoin and J. W. Corbett, Phys. Lett. A **38**, 135–137 (1972).
[11]W. T. Stacy and B. J. Fitzpatrick, J. Appl. Phys. **49**, 4765 (1978).
[12]G Watkins, J. Cryst. Growth **159**, 338–344 (1996).
[13]J. Adey, R. Jones, D. Palmer, P. Briddon, and S. Öberg, Phys. Rev. Lett. **93**, 1–4 (2004).
[14]J Schmidt, K Bothe, D Macdonald, J Adey, R Jones, and D W Palmer, J. Mater. Res. **21**, 5–12 (2006).
[15]L. I. Murin, E. A. Tolkacheva, V. P. Markevich, A. R. Peaker, B. Hamilton, E. Monakhov, B. G. Svensson, J. L. Lindstrom, P. Santos, J. Coutinho, and A. Carvalho, Appl. Phys. Lett. **98**, 182101 (2011).
[16]B. G. Svensson, K.-H. Ryden, and B. M. S. Lewerentz, J. Appl. Phys. **66**, 1699 (1989).
[17]T. Hiyoshi and T. Kimoto, Appl. Phys. Express **2**, 91101 (2009).
[18]T. Hiyoshi and T. Kimoto, Appl. Phys. Express **2**, 41101 (2009).
[19]L. S. Løvlie, L. Vines, and B. G. Svensson, Mater. Sci. Forum **645–648**, 431–434 (2010).
[20]This is a simulation software package, located at http://www.srim.org, authored by J. F. Ziegler.
[21]A. A. Istratov, J. Appl. Phys. **82**, 2965 (1997).
[22]J. P. Doyle, M. K. Linnarsson, P. Pellegrino, N. Keskitalo, B. G. Svensson, A. Schöner, N. Nordell, and J. L. Lindström, J. Appl. Phys. **84**, 1354 (1998).

[23]C. Hemmingsson, N. T. Son, O. Kordina, J. P. Bergman, E. Janzen, J. L. Lindstrom, S. Savage, and N. Nordell, J. Appl. Phys. **81**, 6155 (1997).
[24]K. Danno and T. Kimoto, J. Appl. Phys. **100**, 113728 (2006).
[25]K. Fujihira, T. Kimoto, and H. Matsunami, Appl. Phys. Lett. **80**, 1586 (2002).
[26]T. Kimoto, K. Hashimoto, and H. Matsunami, Jpn. J. Appl. Phys., Part 1 **42**, 7294–7295 (2003).
[27]T. Kimoto, S. Nakazawa, K. Hashimoto, and H. Matsunami, Appl. Phys. Lett. **79**, 2761 (2001).
[28]I. Pintilie, L. Pintilie, K. Irmscher, and B. Thomas, Appl. Phys. Lett. **81**, 4841 (2002).
[29]S. Sasaki, K. Kawahara, G. Feng, G. Alfieri, and T. Kimoto, J. Appl. Phys. **109**, 013705 (2011).
[30]L. Storasta and H. Tsuchida, Appl. Phys. Lett. **90**, 062116 (2007).
[31]B. G. Svensson, C. Jagadish, A. Hallén, and J. Lalita, Phys. Rev. B **55**, 10498–10507 (1997).
[32]M. V. S. Chandrashekhar, C. I. Thomas, and M. G. Spencer, Appl. Phys. Lett. **89**, 042113 (2006).
[33]B. G. Svensson, B. Mohadjeri, A. Hallen, J. H. Svensson, and W. Corbett, Phys. Rev. B **43**, 2292–2298 (1991).
[34]P. Pellegrino, P. Lévêque, J. Lalita, A. Hallén, C. Jagadish, and B. Svensson, Phys. Rev. B **64**, 1–10 (2001).
[35]H. Lendenmann, F. Dahlquist, N. Johansson, R. Söderholm, P. Åke Nilsson, P. Bergman, and P. Skytt, Mater. Sci. Forum **353–356**, 727–730 (2001).
[36]P. Bergman, H. Lendenmann, P. Åke Nilsson, U. Lindefelt, and P. Skytt, Mater. Sci. Forum **353–356**, 299–302 (2001).
[37]A. Galeckas, J. Linnros, and P. Pirouz, Appl. Phys. Lett. **81**, 883 (2002).
[38]A. Galeckas, J. Linnros, and P. Pirouz, Phys. Rev. Lett. **96**, 1–4 (2006).
[39]J. D. Caldwell, K. X. Liu, M. J. Tadjer, O. J. Glembocki, R. E. Stahlbush, K. D. Hobart, and F. Kub, J. Electron. Mater. **36**, 318–323 (2007).